Study of Structural and Optical Properties of 2D Organic-Inorganic Perovskites based on Triphenylphosphine

Soghra Mirershadi[*1], Saeid Maleki[2]

[1]Department of Engineering Sciences, Faculty of Advanced Technologies, University of Mohaghegh Ardabili, Namin, Iran

[2]Department of Chemistry, Faculty of Sciences, University of Mohaghegh Ardabili, Ardabil, Iran

(Received 11 Nov. 2021; Final revised received 15 Feb. 2022)

Abstract

In recent years, three-dimensional hybrid perovskites ($CH_3NH_3PbX_3$) with X=I, Br, and Cl have raised great attention due to their facile production methods and encouraging energy conversion efficiency in solar cells based on perovskite. A majority of the systematic studies on the regulation of the bandgap in the family of organolead halide perovskites have focused on changing the compositions of halogens. However, the organic portion can provide a wider structural diversity in bandgap and dimensionality in perovskite structures. Thus, Investigation of the structural and optical properties of organic-inorganic perovskites by changing the organic portion seems to be necessary. The main focus of this work is the tetraphenylphosphonium substitutions at the organic portion in the hybrid perovskite structures. In this paper, the fabrication of organic−inorganic hybrid perovskite TPP_2PbX_4, (TPP = $P(C_6H_5)_4$; X = Cl), is reported. The synthesis method, crystal structure, and optical behavior of the synthesized perovskites were investigated. The organic cation effect on the optical properties and bandgap tuning were studied experimentally. The remarkable electronics and optical properties of 2D perovskite structures could provide a different perspective and suggest the potential of these materials for photonics applications.

Keywords: 2D layered hybrids, Perovskites, Tetraphenylphosphonium, Bandgap tuning.

[1]***Corresponding author:*** *Soghra Mirershadi, Department of Engineering Sciences, Faculty of Advanced Technologies, University of Mohaghegh Ardabili, Namin, PO Box 179, Iran. Email:s.mirershadi@uma.ac.ir*

Introduction

In recent years, hybrid organic-inorganic halide materials have developed as excellent candidates for optoelectronic applications, including solar cells [1], light-emitting diodes (LED) [2], lasers [3], and photodetectors [4-7]. Due to their remarkable optoelectronic properties, low-temperature solution applicability, and broad adjustability of their chemical compositions, crystal, and electronic structures hybrid halides have become the focus of researchers worldwide [6]. Among hybrid materials, the perovskite $MAPbI_3$ ($MA = CH_3NH_3$) and its other Pb and Sn derivatives are the most widely studied types due to their performances in high-yield solar cells [8, 9]. Because of the compositional and structural adjustability of hybrid halide A−B−X materials (A = organic cation, B = metal cation, X = halide anion), theoretically, various substitutions can perform at each A, B, and X sites. Change of the organic cation size via A-site substitution gives control over the material's dimensionality, which can be altered from 0D cluster compounds to 3D networks[10].

Moreover, to the size effects, substitutions of the B and X sites allow fine adjustment of the electronic structure and optoelectronic properties since the B and X element states are the main contributors to the states around the Fermi level [11,12]. Through controlling the structural dimensionality and chemical compositions one can design organic-inorganic halides for definite applications including materials for lighting [13,14] and scintillator applications [15-19]. Large band gaps and highly localized charges with extraordinarily high exciton binding energies and stable excitonic emission can be realized in low-dimensional hybrid organic-inorganic materials [20-22]. Excitons (a bound pair of an excited electron and a hole) in inorganic semiconductors, called Wannier excitons, typically have large radii (30−100 Å) and low binding energies (10−30 meV) in the order of kBT at room temperature (∼26 meV).

Charge transport and emission in such systems are typically nonexcitonic; i.e., excitons are broken apart at room temperature into free charge carriers, and the emission from the recombination of the delocalized charges produces lower light output [23, 24]. By selectively combining organic and inorganic components, exciton binding energies (60−545 meV) and radii (22.9−6.2 Å) can be tuned over a broad range in hybrid materials [6, 21, 22]. Decay of stable excitons via recombination of the electron−hole pair results in spontaneous light emission, which can be used for lighting and high-light-yield scintillator applications. To obtain large bandgap materials with high exciton binding energies and localized charges, a low electronegativity B metal element, such as Cd (1.69),[25]can be paired with halogen elements in hybrid organic-inorganic halides[26].

In this work, a systematic study of prospective scintillator material TPP_2PbX_4 ($TPP = P(C_6H_5)_4$; X = Cl) were reported, and their morphology and optical band structure were investigated under powder

x-ray diffraction study, band structure calculation, thermal gravimetric analysis (TGA), differential scanning calorimetry (DSC), inductively coupled plasma (ICP).

Experimental

Material

Chemicals used in this study and the companies they were purchased from are listed as: (i) tetraphenylphosphoniumchloride, 99%, Sigma-Aldrich; (ii) Lead(II) chloride, ($PbCl_2$, Merck-Schuchardt); (iii) absolute ethanol, 200 proof; (ix) diethyl ether, 98%, Alfa Aesar; (x) benzene, >99.9% HPLC grade, Aldrich; (xi) N,N-dimethylformamide(DMF), 99%, Fisher.

Method

To study the hybrid structures, at first,TPP_2PbX_4 (TPP = $P(C_6H_5)_4$; X = Cl) structure was synthesized. 0.002 mol Tetraphenylphosphoniumcholoride and 0.001 mol Lead (II)chloride were separately dissolved in deionized water. Then the solution of Tetraphenylphosphoniumcholoride was added, dropwise, to a cooled (0°C) solution of Lead (II)chloride under vigorous stirring and was allowed to mix for up to 0.5 h. The excess solvent was evaporated and removed from samples in one week at room temperature on a watch glass, and then, white crystals were formed [27-30].

Characterization techniques

The crystal structure and Bragg reflections of TPP_2PbX_4 (TPP = $P(C_6H_5)_4$; X = Cl)hybrids were characterized by x-ray diffraction (XRD) (Cu Ka X-ray radiation source) with 2θ within the range of 2° –70°. The scanning speed and step intervals were 1°/min and 0.02°, respectively. The optical properties were studied through optical absorption. UV–visible optical absorption is measured with (Sinco S4100) spectrophotometer, in the range of 200 to 800 nm, at room temperature. Thermal gravimetric analysis (TGA) with STA PT1000 from Linseis Inc. was used to evaluate the thermal stability of the structures and the quality of the perovskites. Simultaneous inductively coupled plasma optical emission spectrometry (ICP-OES 730-ES, Varian) was employed to evaluate the concentration of the element in the perovskite structures.

Results and discussion

The XRD spectra of the synthesized TPP_2PbX_4 (TPP = $P(C_6H_5)_4$; X = Cl) organic-inorganic hybrid are shown in Figure 1. Data analysis shows that the peaks seen in Figure 1 are related to the hybrid structure of TPP_2PbX_4 with the Miller planes shown in Figure 1. Strong peaks at 12.77, 14.00, 15.85, 19.08, 20.00, and 21.75, corresponding to (100), (110), (200), (210), (220), and (300) planes,

confirm the formation of a cubic perovskite structure. The peaks agree with reported data in the literature [27, 28].
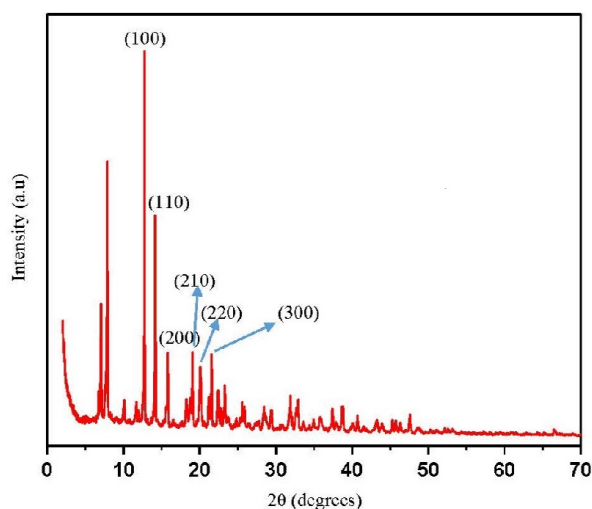
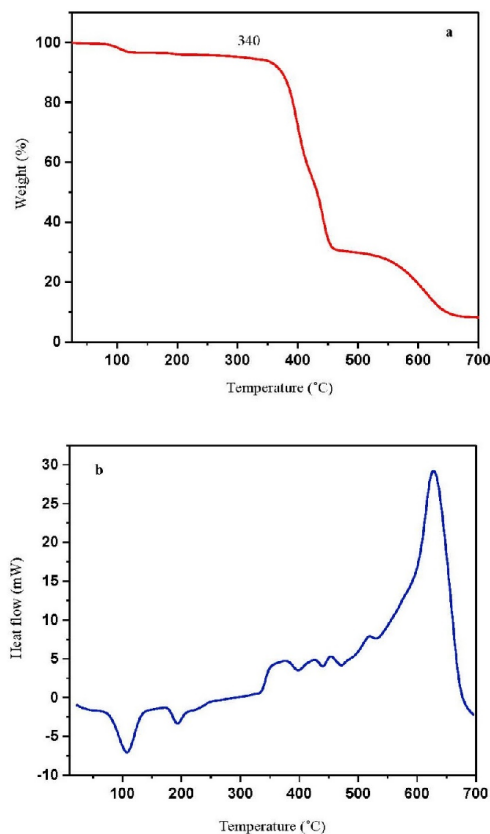**Figure 1.** XRD pattern of the TPP_2PbCl_4 Perovskites.

The elemental composition of any nanomaterial is an essential piece of information for its chemical categorization. Usually, quantitative analyses were performed using inductively coupled plasma (ICP) with optical emission spectrometry (OES) to detect and determine extracted elements. In this work, ICP-OES analysis was employed to determine the elemental composition of the TPP_2PbX_4 (TPP = $P(C_6H_5)_4$; X = Cl) organic-inorganic hybrid perovskite. The results are summarized in Table 1. The difference in the quantity of the elements in experimental and theory indicates that the crystal was formed with defects.

Table1. The results of ICP analysis for the TPP_2PbCl_4 perovskite.

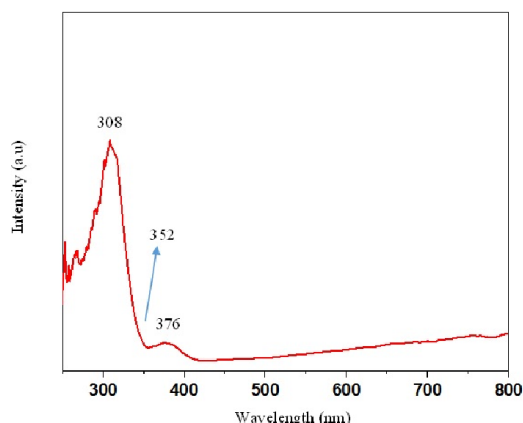| TPP_2PbCl_4 perovskite	% Pb	% p
Experimental	22.38	4.17
Theoretical	20.17	6.03

A thermal analysis method was also used to evaluate the thermal stability of the synthesized structures. In synthesizing the perovskite structures, the reaction temperature with oxygen in the environment is different for each structure. TGA analysis can help to understand the type and amount of these compounds. According to the TGA diagram in Figure 2a, the mass change from temperature 140 °C to 460 °C is about 64.0%, and from the temperature of 460 °C to 700 °C, is about 22.5%. It should be noted that by comparing the TGA results of the TPP_2PbCl_4 in Figure 2a

with the synthesized samples with iron and other organic cations, such as butylamine, and phenethylamine, one can say that the 2D perovskites based on Triphenylphosphine have higher thermal stabilities, compared to the two quasi 2D structures $(BA)_2FeCl_4$ and $(PEA)_2FeCl_4$. The onset, inflection, and offset temperatures determined from Figure 2b represent the temperature at the initial weight loss, the maximum weight loss, and the final weight loss, respectively. The high onset temperatures (350 °C) and high inflection temperature (610 °C) are related to the high thermal stabilities of the TPP_2PbCl_4 structures [29].


Figure 2. (a) TGA results of weight loss vs. temperature of the theTPP_2PbCl_4 Perovskites, (b) DSC traces of the TPP_2PbCl_4 perovskites.

The absorption spectra of the synthesized structures are shown in Figure 3. As seen in this figure, the exciton absorption wavelength is around 352 nm for the TPP_2PbCl_4 perovskite. Assuming that the step-like absorption peak corresponds to the band edge, the bandgap energy (Eg) is roughly estimated to be 3.52 eV.

Figure 3. UV-visible absorption spectra of theTPP$_2$PbCl$_4$ Perovskites.

For further investigation, the optical DRS spectra were used to determine the optical bandgap energy values. Figure 4a shows the emission reflectance spectra of the synthesized hybrids in terms of wavelength. These results indicate the transfer of electrons from the valence band to the conduction band due to the absorption of the incident photon's energy, resulting in the reduction of the light intensity at the mentioned wavelength. As seen in Figure 4(a), the light reflection percentage is reduced in the synthesized structure as the incident photon wavelength decreases from 355 nm to 310 nm.
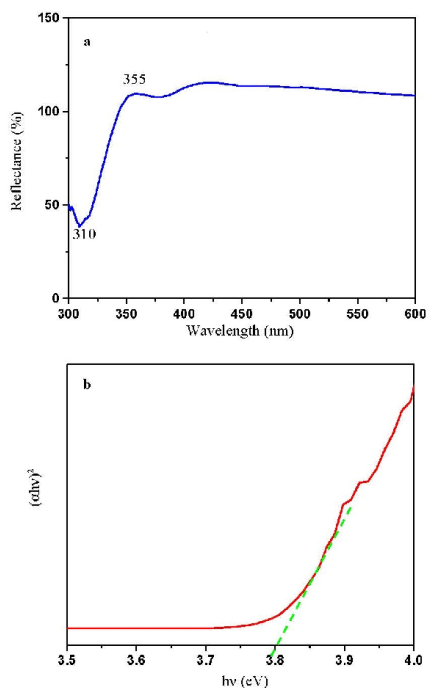
Figure 4.(a) Diffuse reflectance spectra of the TPP$_2$PbCl$_4$ Perovskites, (b)Tauc's plot of $(\alpha h\nu)^2$ as a function of photon energy (hν) for TPP$_2$PbCl$_4$ Perovskites.

53

The $(\alpha h\upsilon)^2$ graph was plotted in terms of the energy of the incident photon ($h\upsilon$) in Figure 4(b). The energy gap for the synthesized structures can be estimated via a tangent line on the diagram in the linear region and are equal to 3.8 electron volts.

Conclusion

In summary, the structural, optical, and electronic properties of TPP_2PbX_4 (TPP = $P(C_6H_5)_4$; X = Cl) 2D hybrid perovskites were investigated in this study. High-quality white crystal was obtained through slow evaporation of water solution of TPP_2PbX_4 at room temperature. X-ray diffraction measurement confirmed a 2D layered perovskite structure for TPP_2PbX_4. Chemical composition in the TPP_2PbX_4 confirmed their air stabilities and the 2D layered perovskite structure. Absorption spectra for this perovskite were investigated. The thermal properties were evaluated using TGA/DSC technique. $(PEA)_2FeCl_4$ hybrid structures were found to display high thermal stabilities. Fortunately, it was demonstrated that these 2D organic-inorganic hybrid perovskites had provided a suitable medium to observe the optical and electronical properties by changing the organic portion in hybrid structures. The ability to tune the emission spectra or optical bandgap through organic cation replacement in perovskite structures is the major advantage of hybrid perovskites. Therefore, this tunability opens a new area of possibilities for perovskite-based optical devices with engineered band structures.

References

[1] D. Bi, W. Tress, M. I. Dar, P. Gao, J. Luo, C. Renevier,K. Schenk, A. Abate, F. Giordano, J. P. Baena, J. D. Decoppet, S. M. Zakeeruddin, M. K. Nazeeruddin, M. Grätzel, A.Hagfeldt, *Sci. Adv.,* 2, e1501170 (2016).

[2] G. Pacchioni, *Nat.Rev.Mater.,* 6, 108 (2021).

[3] S. A. Veldhuis, P. P. Boix, N. Yantara, M. Li, T. C. Sum, N. Mathews, S. G. Mhaisalkar, *Adv. Mater.,* 28, 6804 (2016).

[4] L. Dou, Y. Yang, J. You, Z. Hong, W.H. Chang, G. Li, Y. Yang,*Nat. Commun.,*5, 5404 (2014).

[5] J. S. Manser, J. A. Christians, P. V. Kamat,*Chem. Rev.,* 116, 12956 (2016).

[6] B. Saparov, D. B. Mitzi,*Chem. Rev.,* 116, 4558 (2016).

[7] C. Li, H. Wang, F. Wang, T. Li, M. Xu, H. Wang, Z. Wang, X. Zhan, W. Hu, L. Shen, *Light Sci. Appl.,* 9, 31 (2020).

[8] M. H. Soltani, A. Reyhani, A. Taherkhani, S. Mirershadi, S. Z. Mortazavi, *J Mater Sci: Mater. Electron.,* 32, 15675 (2021).

[9] F. Ebadi, B. Yang, Y. Kim,R. Mohammadpour, N. Taghavinia, A. Hagfeldt,W. Tress, *J. Mater. Chem. A.,*9, 13967 (2021).

[10] S. D. Stranks, H. J. Snaith,*Nat. Nanotechnol.,* 10, 391(2015).

[11] A. H. Slavney, R. W. Smaha, I. C. Smith, A. Jaffe, D. Umeyama, H. I. Karunadasa, *Inorg. Chem.,* 56, 46(2017).

[12] T. T. Tran, J. R. Panella, J. R. Chamorro, J. R. Morey, T. M. McQueen, *Mater. Horiz.,* 4, 688 (2017).

[13] S. Mirershadi, A. Javad, S.A. Ahmadi-Kandjani, *J. Theor. Appl. Phys.,* 13, 133 (2019).

[14] J. H. Heo, S. H. Im, J. H. Noh, T. N. Mandal, C. S. Lim, J. A. Chang, Y. H. Lee, H. I. Kim, A. Sarkar, M. K. Nazeeruddin, M. Grätzel, S. I. Seok, *Nat. Photonics.,* 7, 486 (2013).

[15] S. Yakunin, M. Sytnyk, D. Kriegner, S. Shrestha, M. Richter, G. J. Matt, H. Azimi, C. J. Brabec, J. Stangl, M. V. Kovalenko, W. Heiss, *Nat. Photonics.,*9, 444 (2015).

[16] C. C. Stoumpos, C. D. Malliakas, J. A. Peters, Z. Liu, M. Sebastian, J. Im, T. C. Chasapis, A. C. Wibowo, D. Y. Chung, A. J. Freeman, B. W. Wessels, M. G. Kanatzidis, *Cryst. Growth Des.,* 13, 2722 (2013).

[17] N. Kawano, M. Koshimizu, Y. Sun, N. Yahaba, Y. Fujimoto, T. Yanagida, K. Asai. *J. Phys. Chem. C.,* 118, 9101 (2014).

[18] L. A. Boatner, D. Wisniewski, J. S. Neal, J. O. Ramey, J. A. Kolopus, B. C. Chakoumakos, M. Wisniewska, R. Custelcean, *Appl. Phys. Lett.,* 93, 244104 (2008).

[19] S. A. Vaughn, B. C. Chakoumakos, R. Custelcean, J. O. Ramey, M. D. Smith, L. A. Boatner, H. C. Loye, *Inorg. Chem*., 51, 10503 (2012).

[20] S. Mirershadi, S. Ahmadi-Kandjani, M. S. Zakerhamidi,S. Z. Mortazavi, *Iran. J. Sci. Technol. Trans. Sci.,*41, 873 (2017).

[21] H. Shi, M. H. Du, *Phys. Rev. Appl.,* 3, 054005 (2015).

[22] P. V. Kamat, *Chem. Rev.,* 93, 267 (1993).

[23] K. M. McCall, C. C, Stoumpos, S. S. Kostina, M. G. Kanatzidis, B. W. Wessels, *Chem. Mater.,* 29, 4129 (2017).

[24] B. Saparov, F. Hong, J. P. Sun, H. S. Duan, W. Meng, S. Cameron, I. G. Hill, Y. Yan, D. M. Mitzi,*Chem. Mater.,* 27, 5622 (2015).

[25] A. L. Allred, Electronegativity values from thermochemical data. *J. Inorg. Nucl. Chem.,* 17, 215 (1961).

[26] J. Zaanen, G. A. Sawatzky, J. W. Allen,*Phys. Rev. Lett.,* 55, 418 (1985).

[27] L. Guo, H. Liu, Y. Dai, S. Ouyang, *J. Phys. Chem. Solids,* 7, 68, 1663 (2007).

[28]A. Aisha, A. Naureen, A. Polyakov, P. Rudolf, *APL. mater*, 6, 114206 (2018).

[29]G. Alvarez, A. Conde-Gallardo, H. Montiel, R. Zamorano,*J. Magn. Magn. Mater.* 401, 196 (2016).

[30]H. Tavakkoli, A. Ghaemi, M.Mostofizadeh, *Int. J. Sci. Res.* 2, 340 (2014).

[31]N. Kitazawa, Y. Watanabe, *J. Phys. Chem. Solids.,* 71, 797(2010).

[32]L. Liang, J. Zhang, Y. Zhou, J. Xie, X. Zhang, M. Guan, B. Pan, Y. Xie, *Sci. Rep.,*1936,1(2013).

[33]L. Guo,H. Liu,Y. Dai,Sh. Ouyang, *J. Phys. Chem. Solids.,* 68, 1663 (2007).